STEM CELLS®

STEM CELL TECHNOLOGY: EPIGENETICS, GENOMICS, PROTEOMICS, AND METABONOMICS

Nuclear Transfer-Derived Epiblast Stem Cells Are Transcriptionally and Epigenetically Distinguishable from Their Fertilized-Derived Counterparts

JULIEN MARUOTTI,[a,b,c,d] XIANG PENG DAI,[e] VINCENT BROCHARD,[b,d] LUC JOUNEAU,[b,d] JUN LIU,[f] AMÉLIE BONNET-GARNIER,[b,d] HÉLÈNE JAMMES,[b,d] LUDOVIC VALLIER,[g] I. GABRIELLE M. BRONS,[g] ROGER PEDERSEN,[g] JEAN-PAUL RENARD,[a,b,d] QI ZHOU,[a,e] ALICE JOUNEAU[a,b,d]

[a]Sino-French Laboratory LABIOCEM, Institute of Zoology, Chinese Academy of Sciences, Beijing, China; [b]INRA, UMR 1198 Biologie du Développement et Reproduction, Jouy en Josas, France; [c]Graduate School of Chinese Academy of Sciences, Chinese Academy of Sciences, Beijing, China; [d]ENVA, Maison-Alfort, France; [e]State Key Laboratory of Reproductive Biology, Institute of Zoology, Chinese Academy of Sciences, Beijing, China; [f]Institute of Genetics and Developmental Biology, Chinese Academy of Sciences, Beijing, China; [g]Laboratory for Regenerative Medicine, Department of Surgery, University of Cambridge, Cambridge, United Kingdom

Key Words. Reprogramming • Nuclear transfer • Cloning • Pluripotent stem cells

ABSTRACT

Mouse embryonic pluripotent stem cells can be obtained from the inner cell mass at the blastocyst stage (embryonic stem cells, ESCs) or from the late epiblast of postimplantation embryos (epiblast stem cells, EpiSCs). During normal development, the transition between these two stages is marked by major epigenetic and transcriptional changes including DNA de novo methylation. These modifications represent an epigenetic mark conserved in ESCs and EpiSCs. Pluripotent ESCs derived from blastocysts generated by nuclear transfer (NT) have been shown to be correctly reprogrammed. However, NT embryos frequently undergo abnormal development. In the present study, we have examined whether pluripotent cells could be derived from the epiblast of postimplantation NT embryos and whether the reprogramming process would affect the epigenetic changes occurring at this stage, which could explain abnormal development of NT embryos. We showed that EpiSCs could be derived with the same efficiency from NT embryos and from their fertilized counterparts. However, gene expression profile analyses showed divergence between fertilized- and nuclear transfer-EpiSCs with a surprising bias in the distribution of the differentially expressed genes, 30% of them being localized on chromosome 11. A majority of these genes were downregulated in NT-EpiSCs and imprinted genes represented a significant fraction of them. Notably, analysis of the epigenetic status of a downregulated imprinted gene in NT-EpiSCs revealed complete methylation of the two alleles. Therefore, EpiSCs derived from NT embryos appear to be incorrectly reprogrammed, indicating that abnormal epigenetic marks are imposed on cells in NT embryos during the transition from early to late epiblast. STEM CELLS *2010;28:743–752*

Disclosure of potential conflicts of interest is found at the end of this article.

INTRODUCTION

Mouse embryonic pluripotent cells can be derived from the early epiblast cells within the inner cell mass (ICM) at the blastocyst stage (embryonic stem cells, ESCs) or from the late epiblast of postimplantation embryo (epiblast stem cells [1, 2], EpiSCs). Although these pluripotent stem cells share the same core transcriptional network including the pluripotency factors Oct3/4, Sox2, and Nanog, they differ not only by their culture condition requirements but also by the extent of their contribution to chimeras: only ESCs can integrate

J.M.: conception and design, collection and/or assembly of data, data analysis and interpretation, manuscript writing; X.P.D. and V.B.: provision of study material; J.M. and X.P.D.: contributed equally to this work; L.J. and J.L.: data analysis and interpretation; A.B.: karyotype analysis; H.J.: bisulfite conversion and sequence analysis; L.V.: conception and design, text editing; I.G.M.B. and R.P.: help with EpiSC derivation, scientific advice; Q.Z.: financial and administrative support, scientific advice; J.R.: financial and administrative support, data analysis and interpretation, manuscript writing, final approval of manuscript; A.J.: conception and design, data analysis and interpretation, manuscript writing, final approval of manuscript.

Correspondence: Alice Jouneau, UMR Biologie du Developpement et Reproduction, Bat 230, INRA domaine de Vilvert, 78352 Jouy-en-Josas cedex, France. Telephone: 33 1 34 65 25 68; Fax: 33 1 34 65 23 64; e-mail: alice.jouneau@jouy.inra.fr; or Qi Zhou, Chinese Academy of Sciences, Institute of Zoology, State-Key Laboratory of Reproductive Biology, 1 Beichen West Road, Chaoyang District, Beijing 100101, P.R. China. Telephone: 86-10-64807050; Fax: 86-10-64807316; e-mail: qzhou@ioz.ac.cn Received December 15, 2009; accepted for publication February 16, 2010; first published online in STEM CELLS *EXPRESS* March 3, 2010. 1066-5099/2009/$30.00/0 doi: 10.1002/stem.400

properly within the host blastocyst and contribute to the germline [1, 2]. Moreover, their epigenetic status differs, reflecting the modifications accompanying the transition from naïve epiblast to advanced, pregastrulating epiblast [3, 4]. These modifications include the de novo methylation of the genome and the X-inactivation process [5–8].

Reprogramming somatic nuclear activity through nuclear transfer (NT) has been shown to give rise to fertile adults. It is commonly admitted that low efficiency of successful development is correlated by incomplete or error-prone epigenetic reprogramming. Indeed, chromatin modifications such as histone marks and DNA methylation have been shown to be affected after NT not only in early embryos but also in animals after birth [9–12]. However, several studies have reported that ESCs derived from NT blastocysts (NT-ESCs) are fully pluripotent and have a normal epigenetic status. Moreover, they have been shown to be equivalent to their fertilized (FT) counterparts for their transcriptome, proteome, and miRNA profiles [13–15]. Strikingly, NT-ESCs are derived from blastocysts which frequently exhibit abnormal features in terms of both morphology [16] and transcriptional activities [17]. Moreover, we have shown that defects present in the ICM were mainly responsible for the loss of embryos at periimplantation stages [18]. In view of these results, the similarity of NT-ESCs and FT-ESCs is intriguing and suggests either that the defects in the NT-ICM do not affect derivation of ES cells in vitro or that a normal pattern of gene expression is acquired during the in vitro culture period required to establish ESC lines. Alternatively, but not exclusively, it can be hypothesized that NT-ESCs might be derived from a subset of correctly reprogrammed NT-ICM cells.

Furthermore, most of the early postimplantation NT embryos clearly exhibit abnormal developmental features, originating from defects in both the epiblast and the trophoblast [18, 19]. We therefore decided to derive and to study EpiSCs from NT embryos to examine whether the reprogramming processes affect the maintenance of pluripotency in the postimplantation epiblast and the building of the epigenetic barrier separating ESCs and EpiSCs. Our data show that NT-EpiSCs are transcriptionally and epigenetically different from FT-EpiSCs. This is in contrast to the results obtained with FT-ESCs versus NT-ESCs and suggests that pluripotent cell lines from NT embryos at advanced developmental stages have kept the memory of epigenetic alterations occurring during the in vivo establishment of the epigenetic barrier in the epiblast around the implantation time.

Materials and Methods

Animals

A transgenic mouse line (C57Bl6/J) carrying the gene for green fluorescent protein (GFP) under the control of the GOF18 fragment of the *Oct4* promoter was used. The genetic construction was described elsewhere [20] and mice were kindly provided by Professor Zhangjian (Institute of Genetics and Developmental Biology, Chinese Academy of Sciences).

For nuclear-transfer experiments, oocytes and cumulus donor cells were retrieved from B6D2F1 or from Oct4-GFP B6D2F1 mice. Controls were embryos that were fertilized in vivo (B6D2F1).

All animals were maintained in accordance with the guidelines for the care and use of laboratory animals established by the Beijing Association for Laboratory Animal Science.

Somatic Cell Nuclear Transfer

Nuclear transfer of cumulus nuclei into enucleated oocytes was performed as previously described [21]. Briefly, embryos were reconstructed by injection of cumulus nuclei into enucleated oocytes from superovulated females and then activated with strontium in CZB medium. Embryos were transferred at the two-cell stage into pseudo-pregnant ICR females.

Derivation and Culture of EpiSC Lines

EpiSC lines were derived as previously described [1]: epiblasts from pre-streak/early-streak E7 NT or E6.5 control embryos were cultured in completely defined medium complemented with 20 ng/ml Activin A (R&D Systems Inc., Minneapolis, http://www.rndsystems.com; catalog no. 338-AC) and 12 ng/ml fibroblast growth factor 2 (FGF2; R&D Systems; catalog no. 223-FB). Pluripotent-looking colonies were mechanically picked and expanded before routine passage with collagenase II (Sigma-Aldrich, St. Louis, http://www.sigmaaldrich.com; catalog no. C6885). During picking and the first rounds of passages, culture dishes were coated with 10 μl/ml fibronectin (Chemicon International, Temecula, CA, http://www.chemicon.com; catalog no. FC-010) before switching to fetal calf serum coating. All cell lines were used between passages 10 and 20.

Immunohistochemistry

Alkaline phosphatase staining was performed according to the manufacturer's instructions (Roche Diagnostics, Basel, Switzerland, http://www.roche-applied-science.com; catalog no. 11681451001). For immunofluorescence, outgrowths, and EpiSCs were fixed in 4% paraformaldehyde at 4°C overnight. They were then permeabilized with 0.5% Triton X-100 for 1 hour at room temperature, before blocking with 2% bovine serum albumin in phosphate buffered saline. Incubation was carried out overnight at 4°C with the following antibodies: goat α-Oct4 (monoclonal 1:100), rabbit α-Sox2 (monoclonal 1:500), and mouse α-SSEA-I (monoclonal 1:75) were from Santa Cruz Biotechnology Inc. (Santa Cruz, CA, http://www.scbt.com); rabbit α-Nanog (monoclonal 1:100) was from Chemicon International. Secondary antibodies (FITC or Cy5-conjugate from ZhongShan Biotechnology Co., Ltd, Beijing, PRC) were used for detection as appropriate. Nuclei were counterstained with propidium iodide (Sigma-Aldrich). Observations were made with an epifluorescence microscope (Leica, Heerbrugg, Switzerland, http://www.leica.com) or a LSM 510 META confocal microscope (Carl Zeiss, Jena, Germany, http://www.zeiss.com).

Bisulfite Genomic Sequencing

DNA was extracted from cumulus cells, E13.5 fetuses, and EpiSC lines. Bisulfite treatment was performed as previously described [22]. Primers for *Snrpn*/*Snurf* and polymerase chain reaction (PCR) conditions used to amplify products from bisulfite-treated DNA were described elsewhere [23]. The amplified region corresponds to the DMR1 encompassing the transcription start site and containing 16 CpG residues. Amplified products were sequenced by Cogenics (Beckman Coulter Genomics, Takeley, United Kingdom, https://www.cogenicsonline.com)

Reverse Transcription-Polymerase Chain Reaction (RT-PCR) and Quantitative RT-PCR Analysis

Total RNAs were extracted using the RNeasy minikit (Qiagen, Hilden, Germany, http://www1.qiagen.com) with DNaseI treatment and reverse-transcribed with superscript II reverse transcriptase (Invitrogen, Carlsbad, CA, http://www.invitrogen.com). FT- and NT-ESC samples were obtained from a previous study [24]. PCR was done as previously described [1]. Real-time PCR was run in triplicate on a Step One plus (Applied BioSystems, Foster City, CA, http://www.appliedbiosystems.com) and expression data normalized by the expression level of β-Actin (*Actb*). Primer pairs for quantitative RT-PCR were all from Primer Bank (http://pga.mgh.harvard.edu/primerbank): *Snrpn*/*Snurf* (ID 15029532a1), *Ndn* (ID 31981598a1), *Peg3* (ID 6561146a1), *Krt19* (ID 6680606a1), and *Gusb* (ID 6754098a1) except for *Actb* (forward: 5′-GCTCTGGCTCCTAGCACCAT-3′; reverse: 5′-GCCAC CGATCCACACCGCGT-3′).

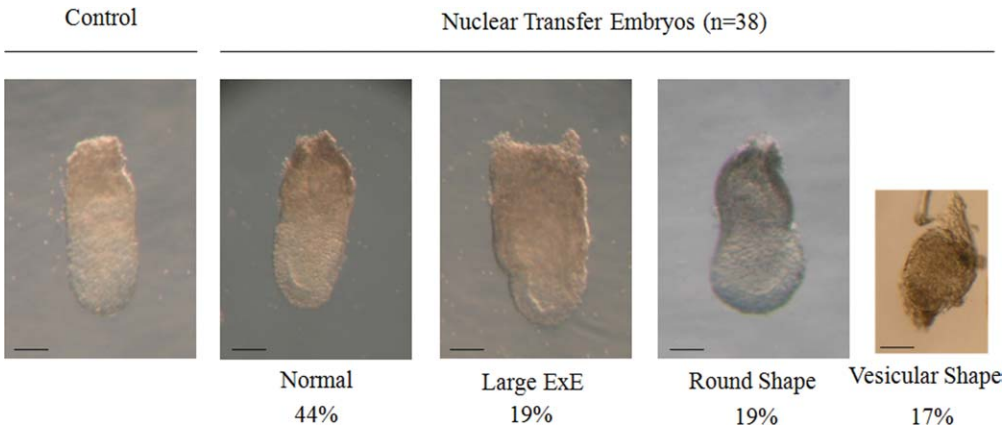

Figure 1. Morphology of fertilized (FT) and nuclear transfer (NT) embryos. Bright-field image of FT and NT-derived embryos at prestreak stage (scale bar: 100 μm) and distribution of the different morphologies among NT embryos. FT embryos were dissected at E6.5 and NT embryos were dissected at E7. Abbreviation: large ExE, large extraembryonic ectoderm.

Mitotic Index Determination

FT and NT outgrowths were stained for Oct4 and counterstained with propidium iodide. Optical sectioning was carried out using a confocal microscope (LSM 510 META; Carl Zeiss) and the number of mitotic figures was counted on each slice using ImageJ software (http://rsb.info.nih.gov/ij/Java1.3.1_13). A total of 750-1,000 cells across different optical sections were counted in each sample.

5-Bromo-2′-deoxy-uridine Incorporation Assay

Cell proliferation assays were carried out according to the manufacturer's instruction (Roche Diagnostics; 5-Bromo-2′-deoxyuridine [BrdU] labeling kit, catalog no. 11 296 736 001). For each cell line (passages 10-15), cells from three independent biological repeats were labeled and about 250 cells counted in each.

Gene Expression Analysis Using Microarray

For each EpiSC line, total RNAs were extracted from two to three independent biological repeats. For male and female prestreak embryos, total RNAs were extracted from 3 pools of 10 embryos, each of the same sex. Hybridizations were performed using the Illumina array Mouse WG-6 V2.0 expression BeadChip. Raw data were analyzed using BeadStudio v3 software (Illumina Inc., San Diego, CA, http://www.illumina.com). Values were normalized and log2 transformed under R software. To obtain the list of differentially expressed probes, we used a Student's t test (limma R package, 2004) and p values were adjusted using the Benjamini-Hochberg method for false discovery rate control [25]. Transcriptomic data are accessible in the Gene Expression Omnibus with the accession number GSE17402.

Embryoid Body Formation

Embryoid bodies (EBs) were produced as described previously [1]. Briefly, floating EpiSC clumps were cultured for 6 days in Dulbecco's modified Eagle's medium with 10% fetal calf serum. Resulting EBs were plated on 0.1% gelatin-coated dishes and cultured for 10 days.

Statistical Analysis

Statistical analyses were carried out using SPSS 13.0. χ^2, Kruskal-Wallis, and ANOVA tests were used when appropriate, with a significant value of $p < .05$.

Results

FT- and NT-EpiSC Are Similar in Terms of Marker Expression and In Vitro Differentiation

Pre-streak/early-streak NT embryos obtained from somatic cell nuclear transfer (SCNT) were dissected at E7 and grouped according to their morphological aspect (Fig. 1). The different classes of morphology were previously defined using ESCs as donor nuclei [18]. With use of the same criteria, 16 SCNT embryos out of 38 (44%) exhibited morphology similar to that of controls and belonged to the "normal" class. Nineteen percent of NT embryo epiblasts had a size inferior to their extraembryonic ectoderm (ExE) and this group was defined as "large extraembryonic ectoderm" (large ExE) embryos. 19% of the epiblasts were more spherical than elongated and wider than the ExE and were classed in the "round shape" category. Finally, 17% of the NT embryos displayed a very perturbed morphology with no clear distinction between the embryonic and extraembryonic compartment and were consequently considered as belonging to the "vesicular shape" category.

Epiblasts could be successfully isolated from all the different NT-embryo categories except for the vesicular shape category. The resulting clump of cells was grown in a defined medium supplemented with Activin and FGF2 [1] until it formed an outgrowth from which pluripotent colonies were identified using morphological criteria (tightly packed colonies of smooth appearance, with large nuclei). These colonies were picked and expanded in the same culture conditions. After several rounds of mechanical passage, stable and pluripotent-looking cell lines were obtained with a similar efficiency from FT and NT embryos (Table 1). Both kinds of cell lines were passaged every 2 or 3 days and were morphologically similar (Fig. 2A).

When the last type of embryos (vesicular shape) was cultured, they rarely formed an outgrowth and did not give rise to any EpiSC line. Immunofluorescence analysis indicated that no cell of outgrowth from vesicular shape embryos expressed Oct4, a key marker of pluripotency [26] (data not shown).

Three FT-EpiSC lines (FT.1, FT.2, and FT.3) and three NT-EpiSC lines (NT.1 and NT.2 derived from normal embryo, NT-LE derived from large ExE embryo) were selected for further analyses. FT and NT lines expressed markers of pluripotency including Oct4, Nanog, Sox2, and

Table 1. Efficiency of derivation of EpiSC lines from FT and NT embryos

Type of embryo	No. of epiblasts	No. of outgrowths	No. of lines derived	Embryo morphology	Rate[b] (%)
FT	18	18	5	normal	27.8
NT	17	15[a]	5	2 Normal, 2 large ExE, 1 round shape	33.3

No statistical difference was found in the derivation efficiency between fertilized and NT EpiSC.
[a]Two epiblasts belonged to the vesicular shape class and did not develop into an outgrowth.
[b]The rate is calculated from the ratio between the number of derived lines and the number of outgrowths.Abbreviations: EpiSC, epiblast stem cell; ExE, extraembryonic ectoderm; FT, fertilized; NT, nuclear transfer.

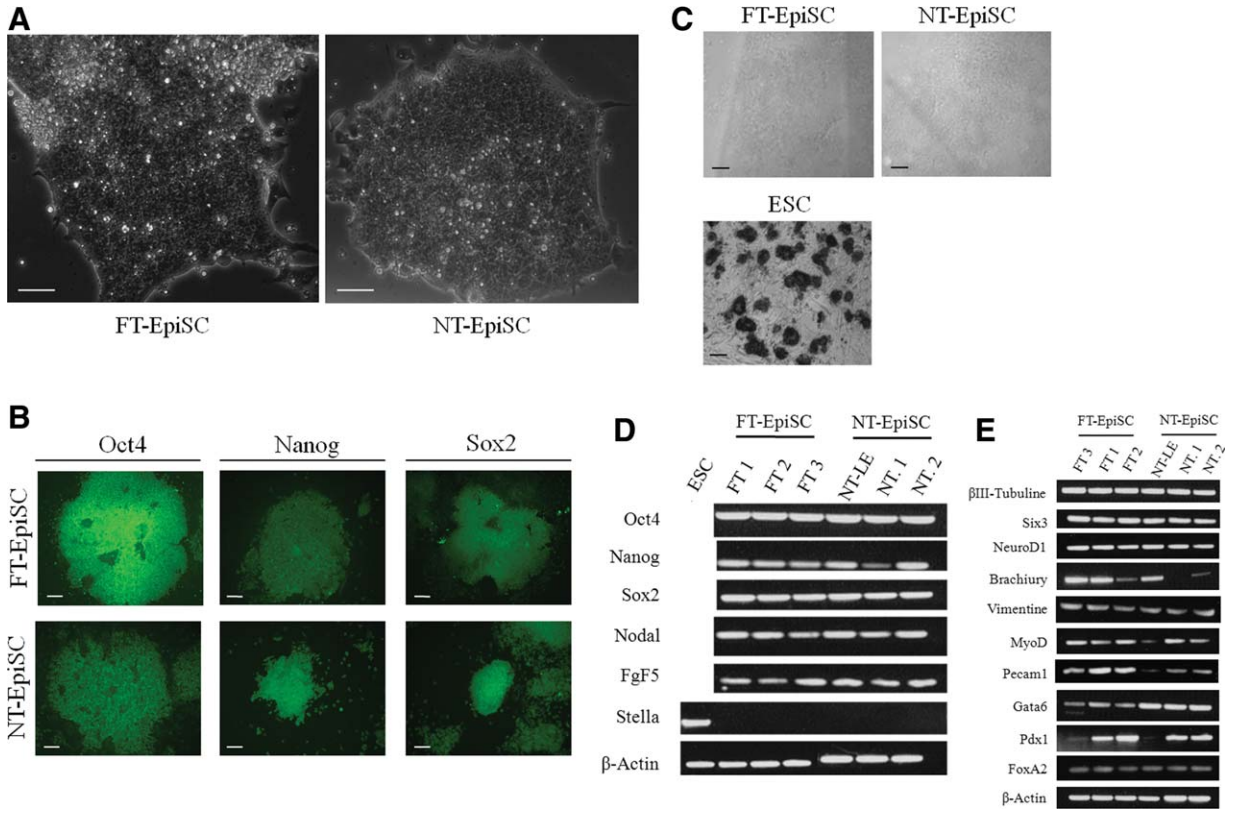

Figure 2. Characterization of derived EpiSC lines. (**A**): Phase contrast images of FT- and NT-EpiSCs (scale bar: 50 μm). (**B**): Immunofluorescence staining of FT- and NT-EpiSC for Oct4, Nanog, and Sox2 as indicated (scale bar: 10 μm). (**C**): Alkaline phosphatase staining of FT- and NT-EpiSCs and mouse ESCs (scale bar: 10 μm). EpiSCs are alkaline phosphatase negative, as expected. (**D**): Reverse-transcription-polymerase chain reaction (RT-PCR) analysis of pluripotency and specific markers in FT- and NT-EpiSCs. Mouse ES cells were used as positive control for Stella expression. (**E**): RT-PCR analysis of markers of differentiation in embryoid bodies derived from FT- and NT-EpiSCs and plated for 10 days. Abbreviations: EpiSCs, epiblast stem cell; ESCs, embryonic stem cell; FT, fertilized; NT, nuclear transfer.

SSEA-1 but stained negatively for alkaline phosphatase (Fig. 2B, 2C and data not shown). RT-PCR analyses confirmed the expression of pluripotency markers and epiblast markers such as *FgF5* and *Nodal* in both FT- and NT-EpiSCs (Fig. 2D). As expected, FT- and NT-EpiSCs did not express the germ cell-specific marker *Stella* (Fig. 2D). Taken together, these data indicate that FT- and NT-EpiSCs express markers characterizing EpiSCs [1, 2] and thus validate their embryonic identity.

Importantly, FT- and NT-EpiSCs were able to form EBs that gave rise to various tissues, including fibroblast-like cells, liver-like cells, and beating cells once grown in adherent culture conditions (data not shown). Presence of derivatives of the three primary germ layers was confirmed by RT-PCR analyses, showing that plated EBs from FT- and NT-EpiSCs expressed markers specific for neuronal differentiation (*Tubb3*, *Six3*, and *Neurod1*; Fig. 2E), mesoderm differentiation (*Brachyury* [early mesoderm], *Vimentin* and *Myod1* [myogenic tissues], and *Pecam1* [vascular tissues]; Fig. 2E), and endoderm differentiation (*Gata6*, *Pdx1*, and *Foxa2*; Fig. 2E). Together, these results show that FT- and NT-EpiSC lines are able to differentiate into derivatives of the three primary germ layers in vitro.

FT- and NT-EpiSC Lines Proliferate at the Same Rate

Interestingly, we observed that the mitotic index of a large proportion (41%) of epiblasts from postimplantation cloned embryos significantly differs from controls [18], suggesting that NT- and FT-EpiSCs could have different rates of proliferation. To confirm this hypothesis, we used BrdU incorporation

assays to determine the cell proliferation in the different EpiSC lines. After only 5 minutes of BrdU pulse, 70% of cells were stained in FT and NT lines (supporting information Fig. 1A, 1B), and after 1 hour of BrdU incubation, this percentage rose to 78%. Statistical comparison indicated no significant difference between rates of BrdU incorporation in FT- and NT-EpiSC lines. Therefore, cell proliferation rates are similar between FT- and NT-EpiSCs.

FT and NT Outgrowths Display a Similar Dynamic Pattern of Oct4 Expression

The results described above suggested that the differences in cell proliferation observed between FT and NT epiblasts in vivo were lost in vitro. Therefore, we decided to examine whether these difference were still present when pluripotent primary colonies of EpiSCs were formed at the outgrowth stage. Once plated on fibronectin, isolated epiblasts grew actively and formed an outgrowth in which EpiSC pluripotent primary colonies were easily recognized by their morphology. Oct4 is a key marker of pluripotency [26] expressed in EpiSC lines and lost upon their differentiation [1]. To follow the dynamics of Oct4 expression pattern during the outgrowth phase in FT- and NT-EpiSC line derivation, we used embryos expressing the GFP under the control of the Oct4 promoter [20]. During our observations, we noticed that Oct4-expressing cells always had pluripotent morphology, although the contrary was not always true. Moreover, EpiSC lines were derived only from GFP-positive colonies and never arose from cells negative for Oct4 expression (data not shown).

Two patterns of Oct4 expression were observed (Fig. 3A, 3B) in FT and NT outgrowths: (i) From day 1 to days 3-4 of in vitro culture, there was a progressive decrease of the Oct4-expressing cell population, before its rise during the next 4-8 days, until Oct4-expressing colonies were large enough for picking and subsequent EpiSC derivation. This pattern was followed by 36% (4/11) and 44% (4/9) of FT and NT outgrowths, respectively. (ii) From day 1 to days 3-5 of in vitro culture, the Oct4-expressing cell population progressively disappeared and did not reappear. This happened in 64% (7/11) of the FT outgrowths, versus 56% (5/9) for their NT counterparts. The same distribution within the two patterns was found for the two types of outgrowths. Therefore, the derivation process appears very similar for NT and FT epiblasts.

In Oct4-Expressing Areas, Cell Proliferation Differences Between FT and NT Outgrowths Fade Away During In Vitro Culture

To confirm these observations, we performed immunostaining analyses for the expression of Oct4 and compared the cell proliferation in FT versus NT outgrowths. Since EpiSC lines were derived from Oct4-positive primary colonies within the outgrowths, we decided to define the proliferation rate of this particular cell population. First, the Oct4 expression pattern previously observed in FT and NT outgrowths with the Oct4-GFP construct was confirmed by immunofluorescence after 24 hours, 4 days, and 10 days of in vitro culture (supporting information Fig. 2). Then we used mitotic index to assess cell proliferation. Importantly, preliminary experiments with BrdU were unsuccessful because of the limited penetration of BrdU into the outgrowth inner cells. Two time points were chosen: after 24 hours of in vitro culture, when the outgrowth was mainly composed of Oct4-positive cells and has just started to spread, and after 10 days, when Oct4-positive EpiSC primary colonies were usually picked (supporting information Fig. 2). For each time point, mitotic indexes were determined for 5-10 outgrowths of each type (FT and NT).

Interestingly, when we compared the mitotic index of Oct4-positive and -negative cell colonies within FT and NT outgrowths kept 10 days in culture, we found that in FT and NT outgrowths, Oct4-positive cell colonies had a significantly higher proliferation rate than the Oct4-negative—differentiated—colonies (data not shown). Then we looked at Oct4-expressing areas only and we found that most of the mitotic indexes were comprised between 4% and 12% after 24 hours (Fig. 3C) and between 3% and 8% at 10 days of in vitro culture. The cell proliferation was significantly lower in NT outgrowths (Fig. 4C) after 24 hours of in vitro culture whereas no difference could be detected after 10 days. Consequently, growth deregulations observed in NT epiblasts in vivo [18] could still be detected in vitro after 24 hours of culture, but disappeared after a prolonged period of culture. Since EpiSC derivation efficiency from FT and NT outgrowths was comparable (Table 1), these results reveal the existence of mechanisms by which cell proliferation defects in the Oct4-expressing cells of the NT outgrowths are corrected by in vitro culture.

FT and NT-EpiSCs Are Distinguishable on the Transcriptomic Level

FT- and NT-EpiSC lines could not be distinguished by their self-renewal property or their capacity of differentiation. Therefore, we decided to further characterize NT- and FT-EpiSCs by performing gene expression profiling. However, some of our FT-EpiSC lines were male (namely, FT.1 and FT.2), whereas all the NT lines were female. To exclude sex-related differences from our subsequent analyses, we compared the transcriptomic profile of pre-streak male and female whole embryos: with an adjusted p value $<.05$ for the Student's t test we could not detect differential gene expression between male and female (data not shown). These results reinforced previous studies showing the limited influence of sex on gene expression in ESCs [27]. Then we performed a hierarchical clustering for all six EpiSC lines (Fig. 5A), and surprisingly, individual EpiSC line expression profiles grouped into two main clusters (Fig. 5B). One that included three FT lines plus NT.1 and thus was named "FT-like" and one that comprised NT-LE and NT.2 lines and was named "abnormal". Hence, nuclear transfer-derived embryos seem able to give rise to NT-EpiSC lines that have expression profiles similar to their control counterparts, and also to NT-EpiSC lines that behave differently on the transcriptional level.

Further analyses revealed that 111 (out of 16061) transcripts were significantly (Student t test with $p \leq .05$) up- or downregulated between the two groups. Among them, 80% are downregulated in abnormal NT-EPiSCs. Twenty-five were differentially expressed with a twofold change or more (Table 2). Noteworthy, the most affected transcripts (dysregulations with folds superior to 10) were all downregulated and they all correspond to imprinted genes such as Snrpn/Snrpn upstream reading frame (*Snrpn*/*Snurf*), necdin (*Ndn*), mesoderm-specific transcripts (*Mest*), imprinted and ancient (*Impact*), and paternally expressed 3 (*Peg3*) [28].

In the course of our microarray data analysis, we also found that an unusually high proportion (30%, 32/111) of differentially expressed transcripts originated from genes present on chromosome 11. To confirm this observation, we compared the distribution of the transcripts expressed in EpiSCs (FT or NT) on the 20 pairs of chromosomes to that of the differentially expressed transcripts (Fig. 5D). Statistical analysis (χ^2, $p < 10^{-13}$) confirmed that there was a clear bias in the location of the genes that have a perturbed expression in abnormal NT-EpiSC lines. To test the possibility that the bias was due to a structural defect affecting chromosome

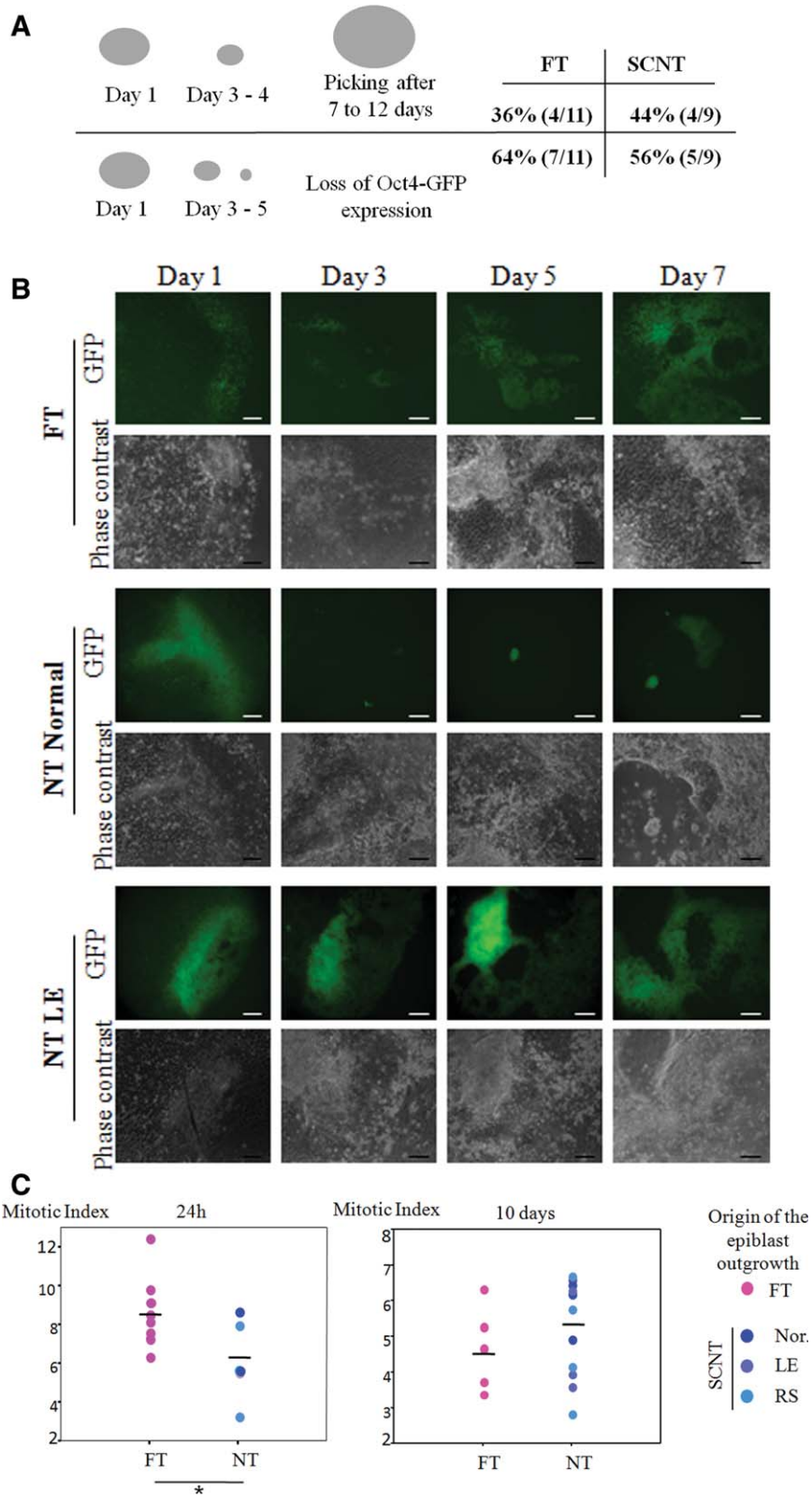

Figure 3. Oct4 expression pattern in FT and NT outgrowths at different time points and Mitotic Index of the Oct4-expressing cell population. (**A**): Diagram depicting the evolution of Oct4-expressing cell population in FT and NT outgrowths. (**B**): Expression of the green fluorescent protein under the control of the Oct4 promoter in FT and NT outgrowths at different time points as indicated (scale bar: 100 μm). Only outgrowths that could be successfully picked for epiblast stem cell derivation are shown. (**C**): The mitotic indexes were calculated in the outgrowths derived from fertilized or NT embryos and represented individually as dot-plots. Bars indicate the mean. *, $p < .05$. Abbreviations: FT, fertilized; GFP, green fluorescent protein; LE, Large ExE embryo; Nor., normal embryo; NT, nuclear transfer; RS, round shape embryo; SCNT, somatic cell nuclear transfer.

11, we analyzed the karyotype of our EpiSC lines after G-banding staining. No obvious anomaly affecting NT-EpiSCs could be detected (supporting information Fig. 2). In addition, genes downregulated in NT-EpiSCs and located on chromosome 11 were mapped along this chromosome excluding that one particular genomic region could have been affected by some subtle structural abnormalities (supporting information Fig. 4).

Finally, these results were confirmed by performing quantitative RT-PCR analyses showing (Fig. 5E) that three

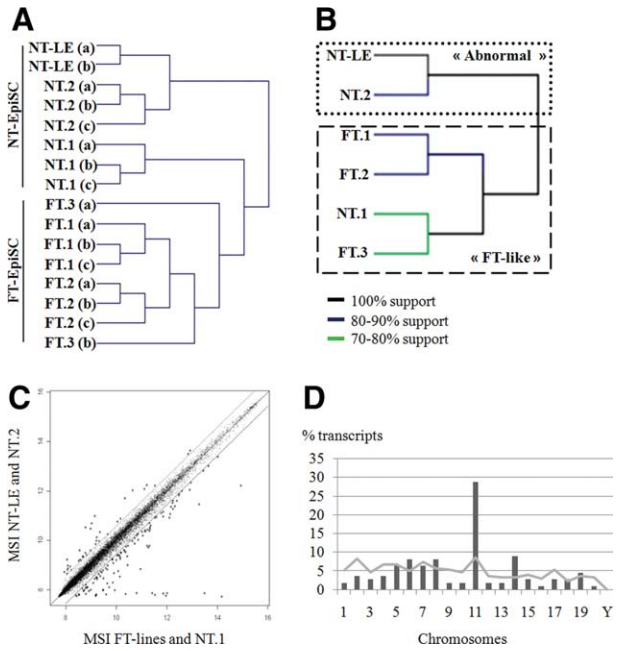

Figure 4. Transcriptomic analysis of FT- and NT-EpiSC lines. (**A**): Hierarchical clustering of EpiSC line expression profiles: sample tree for each biological repeat, named (**a**), (**b**), and (**c**). (**B**): Hierarchical clustering of EpiSC lines expression profiles: sample tree for each line. (**C**): Analysis of expression profiles. MSI of NT-LE and NT.2 lines were plotted against the corresponding MSI of the three FT lines and NT.1. Dotted lines indicate 1.5-fold regulation. Stars indicate transcripts differentially expressed with a 1.5-fold or more change. (**D**): Chromosomal distribution of the transcripts present on the array (gray line) and of the differentially expressed transcripts (gray bars). Abbreviations: EpiSC, epiblast stem cell; FT, fertilized; GFP, green fluorescent protein; LE, Large ExE embryo; MSI, mean signal intensities; NT, nuclear transfer.

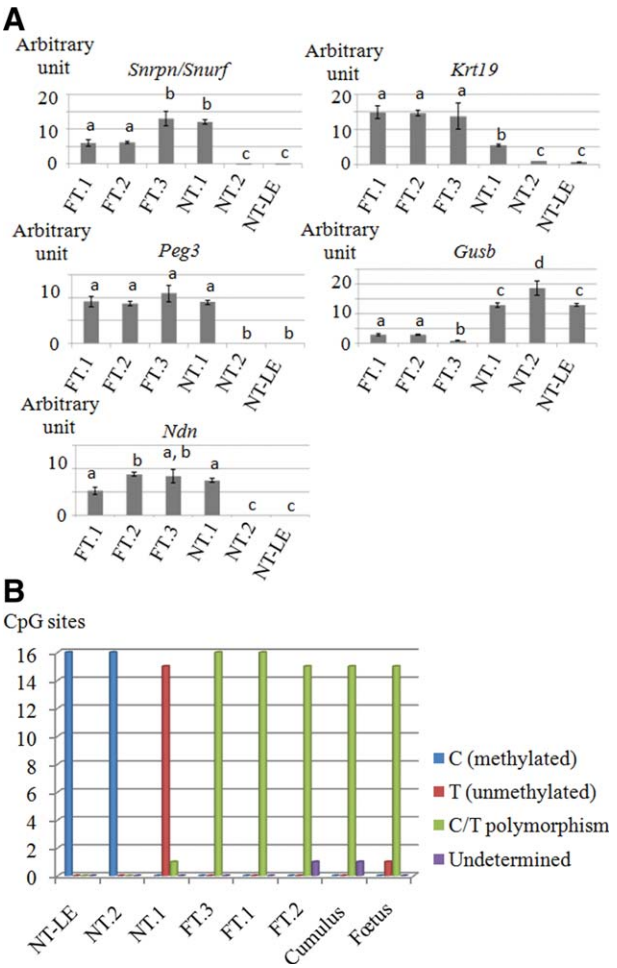

Figure 5. Confirmation of the transcriptomic data by quantitative reverse transcription-polymerase chain reaction (RT-PCR) and DNA methylation analysis of *Snrpn* and *Peg3*. (**A**): Expression levels of selected genes measured by quantitative RT-PCR in the FT- and NT-EpiSC lines. Expression levels with different letters were significantly different ($p < .05$). Bars show the standard deviation. (**B**): DNA methylation analysis of FT- and NT-EpiSC, foetus lines and cumulus cells by bisulfite conversion followed by direct sequencing for *Snrpn*/*Snurf* differentially methylated region 1. Sixteen CpG residues were analyzed: presence of C or T indicates a methylated or unmethylated residue, respectively. Abbreviations: EpiSC, epiblast stem cell; FT, fertilized; NT, nuclear transfer.

imprinted genes, *Snrpn*/*Snurf*, *Ndn*, and *Peg*, were drastically downregulated in NT-LE and NT.2 compared to the FT-like EpiSCs. To further demonstrate that downregulated expression of these imprinted genes was a feature specific to NT-EpiSCs, similar analyses were performed in FT- and NT-ESC lines, showing that the expression of *Peg3* and *Ndn* was normal in these pluripotent cells (supporting information Fig. 5).

We also compared the level of expression of two other dysregylated genes, keratin 19 (*Krt19*) and glucoronidase beta (*Gusb*), by quantitative PCR (Fig. 5A). The results were in accordance with the transcriptomic data, except that NT.1 expression levels were in these cases closer to those of NT.2 and NT-LE than to the FT lines. This result shows that, for at least some genes, NT.1 tends to behave like the other NT-EpiSC lines. It is in accordance with the data from the hierarchical clustering (Fig. 4A), where the cluster comprising the NT.1 biological repeats was branched between the FT lines cluster, and the NT-LE and NT.2 cluster.

Taken together, these results demonstrate that derivation of EpiSCs from NT-embryo transfer can generate pluripotent lines incorrectly reprogrammed and genes located on chromosome 11 appear to be specifically targeted by these reprogramming errors.

FT- and NT-EpiSCs Are Distinguishable on the Epigenetic Level

Imprinted gene expression can be controlled by differentially methylated regions (DMRs) with methylation patterns specific to the maternal or paternal allele [22]. Therefore, we wondered if the perturbation of this methylation pattern could be responsible for the decrease in expression observed in NT-EpiSCs. To validate this hypothesis, we checked the DNA methylation status of one of the most dramatically downregulated imprinted genes, *Snrpn*/*Snurf*. Importantly, this gene is known to have stable and robust imprint that is not affected by environmental parameters such as long-term passages of cells and embryo culture [29]. In sum, the methylation status of the DMR was determined using bisulfite genomic sequencing (Fig. 5B and supporting information Fig. 6) and the presence of polymorphism at all CpG sites was evidenced in the FT-EpiSCs and somatic tissues, in accordance with a methylation of maternal alleles and a demethylation of paternal alleles [30]. However, a loss of polymorphism was found at all CpG positions in NT-EpiSCs. The two abnormal NT-EpiSCs (NT.2 and NT-LE) displayed a full methylation, suggesting a methylation of both parental alleles. By contrast, we observed a nearly complete demethylation of the *Snrpn*/*Snurf* DMR for

Table 2. List of transcripts differentially expressed between EpiSC lines belonging to the abnormal and the FT-like cluster (adjusted p value <.05; fold change ≥ 2)

Symbol	Fold change	Student's t test adjusted p value
Downregulated transcripts in NT.2 and NT-LE		
Snrpn/Snurf	47.9	2.52×10^{-5}
Ndn	16	7.25×10^{-5}
Mest	12.4	2.52×10^{-5}
Impact	11.7	2.14×10^{-3}
Peg3	10.5	2.73×10^{-4}
LOC666403	6.6	.039
Pcsk9	4.3	.010
Stl4	3.1	7.24×10^{-4}
Supt16h	2.9	1.09×10^{-4}
Tomm22	2.9	.028
1700123O20Rik	2.8	4.94×10^{-5}
Adamts9	2.7	.032
C920004C08Rik	2.7	5.71×10^{-4}
LOC100044289	2.7	1.54×10^{-3}
Mkrn3	2.6	1.09×10^{-4}
Krt19	2.6	.016
Rpol-2	2.5	.018
Zfp365	2.3	2.12×10^{-3}
Krt18	2.1	.030
Rpo1-4	2.0	6.76×10^{-3}
Upregulated transcripts in NT.2 and NT-LE		
GusB	2.1	.041
Cdknlc	2.3	4.13×10^{-3}
Prickle4	2.6	.027
Chacl	2.6	5.90×10^{-3}
Cyba	2.8	.033

Abbreviation: EpiSC, epiblast stem cell.

the NT.1 EpiSC line. Therefore, repression of *Snurf*/*Snrpn* expression in the abnormal NT-EpiSCs could be explained by allelic silencing through methylation. Taken together, these results confirm that that there are clear-cut epigenetic differences between FT- and NT-EpiSCs at the single-gene level.

Discussion

Divergences Between EpiSC Derived from NT Embryos or Fertilized Counterparts

In this study, we showed that EpiSCs can be derived with the same efficiency from NT embryos and from fertilized embryos. NT-EpiSCs appear to behave similarly to their FT counterpart as they show the same capacity to proliferate, to express markers of pluripotency such as *Oct4*, *Nanog*, and *Sox2* and to form embryoid bodies capable of differentiating into derivatives of the three germ layers. However, our study also revealed that NT and FT cell lines can also display divergent gene expression profiles. The expression of imprinted genes appears to be particularly variable because of an abnormal methylation pattern of these genomic regions in NT-EpiSCs. This is in striking contrast to the data obtained with ESC lines isolated from NT or FT blastocysts [13, 14]. ESCs and EpiSCs are both obtained from the epiblast, but at different developmental periods, respectively the blastocyst and the pregastrula stages. This suggests that the epigenetic errors imposed on embryonic cells during the process of reprogramming become apparent during the transition from early to late epiblast stages.

Nevertheless, the observation that the mean mitotic index of Oct4-expressing cells in NT-epiblast-derived outgrowths is initially low, but becomes similar to FT epiblast-derived ones after 10 days of culture indicates that an in vitro culture period may be able to correct some of the pre-existing cellular defects induced by the NT procedure. Alternatively, the more correctly reprogrammed pluripotent cells within an outgrowth could gain a selective advantage, and further partial reprogramming could also take place during the in vitro culture. Interestingly, this hypothesis is reinforced by a recent report demonstrating that human-induced pluripotent stem cells (hiPSC) at late passage are closer to hESCs than hiPSCs at early passage [31].

Difference in Imprinted Gene Expression Between "Abnormal" NT-EpiSCs and "FT-like" EpiSCs

Among the transcripts found differentially expressed between "abnormal" and "FT-like" EpiSC, the most dysregulated ones (*Snrpn*/*Snurf*, *Ndn*, *Mest*, *Impact*, *Peg3*) were all from imprinted genes. Such genes can have a perturbed expression in embryos because of incorrect epigenetic reprogramming after NT [32, 33] or in ESCs as a result of accumulated epimutations occurring during in vitro culture [34, 35]. Several reports have shown the epigenetic stability of *Snrpn*/*Snurf*, *Ndn*, and *Peg3* in mESCs [29, 36] and hESCs [37–39] during long-term in vitro culture. After nuclear transfer, disruption of methylation for *Snrpn*/*Snurf* and *Peg3* has been evidenced in NT blastocysts and one NT-ESC line, respectively [32, 36]. Noteworthy, all the reported cases of perturbations affecting imprinted genes show a loss of imprint and biallelic expression, whereas in the present study we report repression of expression in some NT-EpiSCs lines. Moreover, we have been able to correlate the repression of expression of *Snrpn*/*Snurf* with hypermethylation of the DMR region, supporting the view that the paternal allele has been silenced. Data regarding expression of imprinted genes just after implantation in mouse NT embryos are limited and only *Snrpn*/*Snurf*, *Ndn*, and *Peg* have been found to be faithfully expressed in livers of NT pups [40] and also *Mest* at 9.5 dpc [41]. Downregulation of *Snrpn*/*Snurf* and *Ndn* (together with *Mkrn3*) induces postnatal lethality [42], whereas downregulation of *Mest* results in embryonic growth retardation between E15 and E18 [43]. Therefore, concomitant downregulation of these genes by abnormal methylation at the epiblast stage could explain the wave of mortality observed just after implantation and before E7 in NT embryos [18]. Noteworthy, another imprinted gene *Cdkn1c* (*p57*) found upregulated in our abnormal NT-EpiSC has been implicated in embryonic growth retardation and lethality upon a twofold upregulation [44].

In addition, most of the imprinted genes strongly downregulated in abnormal NT-EpiSCs are expressed in the brain [43, 45–48] where some of them are known to play a crucial role in neuronal differentiation [49–55]. Therefore, NT-EpiSC lines could have limited capacity to generate functional neuronal cells and further studies will focus on comparing neuronal differentiation of FT and NT-EpiSCs.

Can Chromosome 11 Be Considered As a Specific Target for Dysregulated Gene Expression in Abnormal NT-EpiSCs?

A puzzling result of our work is the bias that we have evidenced in the genomic localization of the genes found to be downregulated in NT EpiSCs. A significant fraction of these genes are located on chromosome 11, suggesting a specific involvement of this chromosome in abnormal development of early postimplantation NT mouse embryos. Interestingly, predictive analyses have suggested that chromosome 11 is particularly enriched in genes essential for full-term development

[56]. In addition, this chromosome has also been shown in the mouse to be particularly enriched in CpG islands at gene promoters [57]. Together, these data suggest that chromosome 11 could require specific mechanisms to be reprogrammed. At last, our observations provide an additional support to the view that epigenetic more than genetic defects account for the high rate of compromised development observed after nuclear transfer in the mouse once NT blastocysts have formed. We cannot exclude that subtle chromosomic abnormalities affecting chromosome 11, below the level of detection of the G-banding analysis, could have occurred earlier during the process of nuclear transfer itself or in vitro culture [58, 59]. However, the odds of chromosomal rearrangement occurring on the same chromosome in two different NT-EpiSC lines but not in FT-EPiSC lines is rather small. Extension of this result to different genetic backgrounds is underway in our laboratory.

Conclusion

Taken together, our results demonstrate that the reprogramming errors following nuclear transfer perturb the normal process of epigenetic modifications occurring in the developing epiblast. Inappropriate methylation can result in abnormal expression of a large set of genes, one-third of them being located on chromosome 11. Recently, Bao and colleagues have shown that EpiSCs can be reprogrammed into ES-like cells, so called rESCs, showing that some epigenetic barriers could be overcome in vitro [3]. In this regard, our model of EpiSCs derived from NT embryos constitutes an original model to precisely dissect the nature of these epigenetic barriers and their reversibility or irreversibility into rESCs after perturbations such as those induced by nuclear transfer.

Acknowledgments

This project was initiated through a collaborative program raised between INRA and the Chinese Academy of Science (the Labiocem project). It was supported by an internal grant INRA to A.J. (ACI PHASE-2008), a collaborative grant between the Pasteur Institute of Paris, and INRA (PTR no. 331), and two grants from the China National Basic Research Program 2006CB701501 and 2007CB947702. We are grateful to Professor Zhangjian for the gift of the Oct4-GFP mice, to Professor Wang Xiujie for her advice in statistical analysis of the transcriptomic data, and to Nathalie Peynot for her help in QPCR analysis. We thank Bernard Charpentier and Isabelle Bordier from the INRA MRI for their constant support of this project and acknowledge the efficient support of the scientific department of the French Embassy in Beijing and of the Chinese embassy in Paris. Many thanks also to the staff of the animal facilities both in Jouy-en-Josas and Bejing for animal handling. J.M. was supported by a CNRS fellowship and a grant from the ABIES doctorate program.

Disclosure of Potential Conflicts of Interest

The authors indicate no potential conflicts of interest.

References

1 Brons IGM, Smithers LE, Trotter MWB et al. Derivation of pluripotent epiblast stem cells from mammalian embryos. Nature 2007;448: 191–195.
2 Tesar PJ, Chenoweth JG, Brook FA et al. New cell lines from mouse epiblast share defining features with human embryonic stem cells. Nature 2007;448:196–199.
3 Bao S, Tang F, Li X et al. Epigenetic reversion of post-implantation epiblast to pluripotent embryonic stem cells. Nature 2009; 461(7268): 1292–1295.
4 Hayashi K, Lopes SMCdS, Tang F et al. Dynamic equilibrium and heterogeneity of mouse pluripotent stem cells with distinct functional and epigenetic states. Cell Stem Cell 2008;3:391–401.
5 Monk M, Boubelik M, Lehnert S. Temporal and regional changes in DNA methylation in the embryonic, extraembryonic and germ cell lineages during mouse embryo development. Development 1987;99: 371–382.
6 Rossant J, Sanford JP, Chapman VM et al. Undermethylation of structural gene sequences in extraembryonic lineages of the mouse. Dev Biol 1986;117:567–573.
7 Kafri T, Ariel M, Brandeis M et al. Developmental pattern of gene-specific DNA methylation in the mouse embryo and germ line. Genes Dev 1992;6:705–714.
8 Surani MA, Hayashi K, Hajkova P. Genetic and epigenetic regulators of pluripotency. Cell 2007;128:747–762.
9 Wang F, Kou Z, Zhang Y et al. Dynamic reprogramming of histone acetylation and methylation in the first cell cycle of cloned mouse embryos. Biol Reprod 2007;77:1007–1016.
10 Shao GB, Ding HM, Gong AH et al. Inheritance of histone H3 methylation in reprogramming of somatic nuclei following nuclear transfer. J Reprod Dev 2008;54:233–238.
11 Suzuki T, Kondo S, Wakayama T et al. Genome-wide analysis of abnormal H3K9 acetylation in cloned mice. PLoS One 2008;3:e1905.
12 Ohgane J, Wakayama T, Kogo Y et al. DNA methylation variation in cloned mice. Genesis 2001;30:45–50.
13 Brambrink T, Hochedlinger K, Bell G et al. ES cells derived from cloned and fertilized blastocysts are transcriptionally and functionally indistinguishable. Proc Natl Acad Sci U S A 2006;103:933–938.
14 Wakayama S, Jakt ML, Suzuki M et al. Equivalency of nuclear transfer-derived embryonic stem cells to those derived from fertilized mouse blastocysts. Stem Cells 2006;24:2023–2033.
15 Ding J, Guo Y, Liu S et al. Embryonic stem cells derived from somatic cloned and fertilized blastocysts are post-transcriptionally indistinguishable: a MicroRNA and protein profile comparison. Proteomics 2009;9:2711–2721.
16 Boiani M, Eckardt S, Scholer HR et al. Oct4 distribution and level in mouse clones: consequences for pluripotency. Genes Dev 2002;16: 1209–1219.
17 Jincho Y, Sotomaru Y, Kawahara M et al. Identification of genes aberrantly expressed in mouse embryonic stem cell-cloned blastocysts. Biol Reprod 2008;78:568–576.
18 Jouneau A, Zhou Q, Camus A et al. Developmental abnormalities of NT mouse embryos appear early after implantation. Development 2006;133:1597–1607.
19 Miki H, Wakisaka N, Inoue K et al. Embryonic rather than extraembryonic tissues have more impact on the development of placental hyperplasia in cloned mice. Placenta 2009;30:543–546.
20 Yoshimizu T, Sugiyama N, De Felice M et al. Germline-specific expression of the Oct-4/green fluorescent protein (GFP) transgene in mice. Dev Growth Differ 1999;41:675–684.
21 Zhou Q, Renard JP, Le Friec G et al. Generation of fertile cloned rats by regulating oocyte activation. Science 2003;302:1179.
22 Lucifero D, Mertineit C, Clarke HJ et al. Methylation dynamics of imprinted genes in mouse germ cells. Genomics 2002;79:530–538.
23 Liu JH, Zhu JQ, Liang XW et al. Diploid parthenogenetic embryos adopt a maternal-type methylation pattern on both sets of maternal chromosomes. Genomics 2008;91:121–128.
24 Zhao C, Yao R, Hao J et al. Establishment of customized mouse stem cell lines by sequential nuclear transfer. Cell Res 2007;17:80–87.
25 Benjamini Y, Hochberg Y. Controlling the false discovery rate: a practical and powerful approach to multiple testing. J R Stat Soc Ser B 1995;57:289–300.
26 Nichols J, Zevnik B, Anastassiadis K et al. Formation of pluripotent stem cells in the mammalian embryo depends on the POU transcription factor Oct4. Cell 1998;95:379–391.
27 Sharova LV, Sharov AA, Piao Y et al. Global gene expression profiling reveals similarities and differences among mouse pluripotent stem cells of different origins and strains. Dev Biol 2007;307: 446–459.

28 Coan PM, Burton GJ, Ferguson-Smith AC. Imprinted genes in the placenta–a review. Placenta 2005;26 Suppl A:S10–S20.
29 Schumacher A, Doerfler W. Influence of in vitro manipulation on the stability of methylation patterns in the Snurf/Snrpn-imprinting region in mouse embryonic stem cells. Nucleic Acids Res 2004;32: 1566–1576.
30 Szabó PE, Mann JR. Allele-specific expression and total expression levels of imprinted genes during early mouse development: implications for imprinting mechanisms. Genes Dev 1995;9:3097–3108.
31 Chin MH, Mason MJ, Xie W et al. Induced pluripotent stem cells and embryonic stem cells are distinguished by gene expression signatures. Cell Stem Cell 2009;5:111–123.
32 Mann MR, Chung YG, Nolen LD et al. Disruption of imprinted gene methylation and expression in cloned preimplantation stage mouse embryos. Biol Reprod 2003;69:902–914.
33 Suzuki J Jr, Therrien J, Filion F et al. In vitro culture and somatic cell nuclear transfer affect imprinting of SNRPN gene in pre- and post-implantation stages of development in cattle. Bmc Dev Biol 2009;9:9.
34 Humpherys D, Eggan K, Akutsu H et al. Epigenetic instability in ES cells and cloned mice. Science 2001;293:95–97.
35 Dean W, Bowden L, Aitchison A et al. Altered imprinted gene methylation and expression in completely ES cell-derived mouse fetuses: association with aberrant phenotypes. Development 1998;125: 2273–2282.
36 Chang G, Liu S, Wang F et al. Differential methylation status of imprinted genes in nuclear transfer derived ES (NT-ES) cells. Genomics 2009;93:112–119.
37 Rugg-Gunn PJ, Ferguson-Smith AC, Pedersen RA. Epigenetic status of human embryonic stem cells. Nat Genet 2005;37:585–587.
38 Adewumi O, Aflatoonian B, Ahrlund-Richter L et al. Characterization of human embryonic stem cell lines by the International Stem Cell Initiative. Nat Biotechnol 2007;25:803–816.
39 Rugg-Gunn PJ, Ferguson-Smith AC, Pedersen RA. Status of genomic imprinting in human embryonic stem cells as revealed by a large cohort of independently derived and maintained lines. Hum Mol Genet 2007;16 Spec No. 2:R243–R251.
40 Humpherys D, Eggan K, Akutsu H et al. Abnormal gene expression in cloned mice derived from embryonic stem cell and cumulus cell nuclei. Proc Natl Acad Sci U S A 2002;99:12889–12894.
41 Inoue K, Kohda T, Lee J et al. Faithful expression of imprinted genes in cloned mice. Science 2002;295:297.
42 Yang T, Adamson TE, Resnick JL et al. A mouse model for Prader-Willi syndrome imprinting-centre mutations. Nat Genet 1998;19: 25–31.
43 Lefebvre L, Viville S, Barton SC et al. Abnormal maternal behaviour and growth retardation associated with loss of the imprinted gene Mest. Nat Genet 1998;20:163–169.
44 Andrews SC, Wood MD, Tunster SJ et al. Cdkn1c (p57Kip2) is the major regulator of embryonic growth within its imprinted domain on mouse distal chromosome 7. Bmc Dev Biol 2007;7:53.
45 Aizawa T, Maruyama K, Kondo H et al. Expression of necdin, an embryonal carcinoma-derived nuclear protein, in developing mouse brain. Brain Res Dev Brain Res 1992;68:265–274.
46 Grimaldi K, Horn DA, Hudson LD et al. Expression of the SmN splicing protein is developmentally regulated in the rodent brain but not in the rodent heart. Dev Biol 1993;156:319–323.
47 Hagiwara Y, Hirai M, Nishiyama K et al. Screening for imprinted genes by allelic message display: identification of a paternally expressed gene impact on mouse chromosome 18. Proc Nat Acad Sci USA 1997;94:9249–9254.
48 Relaix F, Weng X, Marazzi G et al. Pw1, a novel zinc finger gene implicated in the myogenic and neuronal lineages. Dev Biol 1996; 177:383–396.
49 Takazaki R, Nishimura I, Yoshikawa K. Necdin is required for terminal differentiation and survival of primary dorsal root ganglion neurons. Exp Cell Res 2002;277:220–232.
50 Lee S, Walker CL, Karten B et al. Essential role for the Prader-Willi syndrome protein necdin in axonal outgrowth. Hum Mol Genet 2005; 14:627–637.
51 Muscatelli F, Abrous DN, Massacrier A et al. Disruption of the mouse Necdin gene results in hypothalamic and behavioral alterations reminiscent of the human Prader-Willi syndrome. Hum Mol Genet 2000;9: 3101–3110.
52 Taniura H, Taniguchi N, Hara M et al. Necdin, a postmitotic neuron-specific growth suppressor, interacts with viral transforming proteins and cellular transcription factor E2F1. J Biol Chem 1998;273: 720–728.
53 Kurita M, Kuwajima T, Nishimura I et al. Necdin downregulates CDC2 expression to attenuate neuronal apoptosis. J Neurosci 2006;26: 12003–12013.
54 Kuwajima T, Nishimura I, Yoshikawa K. Necdin promotes GABAergic neuron differentiation in cooperation with Dlx homeodomain proteins. J Neurosci 2006;26:5383–5392.
55 Li L, Keverne EB, Aparicio SA et al. Regulation of maternal behavior and offspring growth by paternally expressed Peg3. Science 1999;284: 330–333.
56 Hentges KE, Pollock DD, Liu B et al. Regional variation in the density of essential genes in mice. PLoS Genet 2007;3:e72.
57 Meissner A, Mikkelsen TS, Gu H et al. Genome-scale DNA methylation maps of pluripotent and differentiated cells. Nature 2008;454: 766–770.
58 Allegrucci C, Young LE. Differences between human embryonic stem cell lines. Hum Reprod Update 2007;13:103–120.
59 Balbach ST, Jauch A, Bohm-Steuer B et al. Chromosome stability differs in cloned mouse embryos and derivative ES cells. Dev Biol 2007; 308:309–321.

See www.StemCells.com for supporting information available online.